Meta-Omics Analysis Reveals Global Distribution of Toxic Pseudo-nitzschia and Enhanced Neurotoxin Production Under Climate Warming

20 authors, including:

Dong Xu
Georgia Institute of Technology
134 PUBLICATIONS   3,058 CITATIONS

Zhuonan Wang
Auburn University
17 PUBLICATIONS   265 CITATIONS

Georgina Lauren Brennan
Aarhus University
33 PUBLICATIONS   876 CITATIONS

Yuqiu Wei
Chinese Academy of Fishery Sciences
76 PUBLICATIONS   797 CITATIONS

Global Change Biology

RESEARCH ARTICLE

Meta-Omics Analysis Reveals Global Distribution of Toxic *Pseudo-nitzschia* and Enhanced Neurotoxin Production Under Climate Warming

Dong Xu[1,2] | Zhuonan Wang[3] | Georgina L. Brennan[4] | Yuqiu Wei[1] | Guanchao Zheng[1] | Qingshan Luan[1] | Xintong Huang[1] | Yanmin Sun[1] | Jia Yang[5] (ID) | Xiaowen Zhang[1] | Ke Sun[1] | Xiao Fan[1] | Yitao Wang[1] | Zhijun Tan[1] | Chris Bowler[6] | Juan J. Pierella Karlusich[7] (ID) | Fei-Xue Fu[8] | Guang Gao[9] (ID) | David A. Hutchins[8] (ID) | Naihao Ye[1,2] (ID)

[1]State Key Laboratory of Mariculture Biobreeding and Sustainable Goods, Yellow Sea Fisheries Research Institute, Chinese Academy of Fishery Sciences, Qingdao, Shandong, China | [2]Laboratory for Marine Fisheries Science and Food Production Processes, Qingdao Marine Science and Technology Center, Qingdao, Shandong, China | [3]Natural Resources Ecology Laboratory, Colorado State University, Fort Collins, Colorado, USA | [4]Department of Ecoscience, Aarhus University, Aarhus, Denmark | [5]Department of Natural Resource Ecology and Management, Oklahoma State University, Stillwater, Oklahoma, USA | [6]Département de Biologie, Institut de Biologie de l'ENS (IBENS), École Normale Supérieure, CNRS, INSERM, Université PSL, Paris, France | [7]Department of Biology, Massachusetts Institute of Technology, Cambridge, Massachusetts, USA | [8]Department of Biological Sciences, University of Southern California, Los Angeles, California, USA | [9]State Key Laboratory of Marine Environmental Science & College of Ocean and Earth Sciences, Xiamen University, Xiamen, China

Correspondence: Guang Gao (guang.gao@xmu.edu.cn) | David A. Hutchins (dahutch@usc.edu) | Naihao Ye (yenh@ysfri.ac.cn)

ABSTRACT

The harmful diatom *Pseudo-nitzschia* produces the neurotoxin domoic acid (DA), threatening human health and seafood safety in a changing climate. However, global patterns of *Pseudo-nitzschia* abundance and the responses of DA production to underlying environmental drivers remain poorly understood, hindering accurate projections of their responses to environmental change. Using global meta-omics data from *Tara* Oceans, alongside field survey data from the Chinese coasts and the Southern Ocean, we present the first evidence that four of the most toxic species—*Pseudo-nitzschia multiseries*, *Pseudo-nitzschia multistriata*, *Pseudo-nitzschia delicatissima*, and *Pseudo-nitzschia pungens*—are prevalent not only in coastal ecosystems but also in open ocean environments, spanning from pole to pole. We identify rising temperatures are recognized as a key driver of *Pseudo-nitzschia*'s spatial distribution, DA production, and biosynthetic metabolism. Global models suggest that by 2100, under the SSP2-4.5 climate scenario, the abundance of *P. multiseries* will increase by approximately 75.4%, while toxin production will be even more significantly enhanced, rising by up to 200.4%. This study significantly expands the known global distribution of these neurotoxin-producing diatoms and predicts their increasing prevalence and toxicity under future global changes.

1 | Introduction

Oceanic harmful algal blooms (HABs) and their associated toxins pose a severe threat to human health (Dai et al. 2023). Across the globe, the frequency, duration, severity, and geographical distribution of HABs are expected to increase across aquatic environments under future global change, becoming a major problem worldwide (Hallegraeff et al. 2021). Among the most hazardous HABs are those formed by the marine diatom genus *Pseudo-nitzschia*, a genus in which 29 of the 71 known species

---

produce the potent neurotoxin domoic acid (DA) (Guiry and Guiry 2021; Lundholm et al. 2009; Supporting Information S1). DA acts as a glutamate analog, affecting the central nervous system and causing severe health impacts (Brunson et al. 2018). High-dose acute DA exposure in humans can cause symptoms of nausea, diarrhea, confusion, and even death. This neurotoxin can also lead to kidney damage, cognitive deficits, and impairment of fetal development in birds and marine mammals through chronic exposure (Lefebvre and Robertson 2010; Scholin et al. 2000). The first toxic *Pseudo-nitzschia multiseries* bloom-associated amnesic shellfish poisoning (ASP) incident was recorded on Prince Edward Island in 1987 when the consumption of blue mussels led to an incident of severe poisoning and human fatalities (Lelong et al. 2012). More recently, the largest recorded toxic *Pseudo-nitzschia* bloom swept the North American Pacific coast in the summer of 2015, causing geographically extensive and prolonged closures of razor clam, rock crab, and Dungeness crab fisheries (McCabe et al. 2016). While such events highlight the diatom's impact, current knowledge of its biogeography is based predominantly on coastal observations (Bates et al. 2018). This focus creates a critical knowledge gap, as the distribution and prevalence of toxigenic *Pseudo-nitzschia* species in the open ocean remain largely unknown, hindering our ability to forecast their global response to climate change.

Overcoming this limitation require new approaches, as accurate identification of phytoplankton taxa, including HAB species, is fundamental to understanding marine biodiversity, primary productivity, and ecosystem responses to environmental change. Traditionally, taxonomic classification has relied on microscopy-based morphological analysis, which provides valuable insights into cell size, structure, and abundance (Wang et al. 2022). However, this approach is limited by its resolution and the need for expert knowledge, particularly when distinguishing morphologically cryptic or fragile taxa (Esenkulova et al. 2020; Rynearson et al. 2020). Advances in molecular techniques have led to the widespread adoption of high-throughput sequencing of marker genes, particularly the 18S rRNA gene, enabling a broader and more sensitive view of community composition (De Vargas et al. 2015). Yet, amplicon-based methods are inherently biased by primer selection and often constrained by short read lengths, impeding species-level resolution and comparative abundance estimates (Wang et al. 2022). Shotgun metagenomics offers a complementary, amplification-free strategy that retrieves both taxonomic and functional information across the eukaryotic microbial community (Obiol et al. 2020). Despite its potential, metagenomics remains analytically complex and cost-intensive, with taxonomic inference limited by incomplete reference databases. As each approach offers distinct strengths and limitations, integrative frameworks combining microscopy, metabarcoding, and metagenomic data are increasingly recognized as essential for comprehensive and accurate phytoplankton community profiling. Meta-omics datasets, for example, *Tara* Oceans (Ibarbalz et al. 2019; Pierella Karlusich et al. 2025) have revolutionized our understanding of marine microbes in the world's ocean and provide opportunities to explore global distribution patterns of the harmful bloom-forming alga *Pseudo-nitzschia*.

Although environmental factors such as rising temperatures, elevated CO_2 levels, and nutrient limitation are thought to promote

growth and DA production by *Pseudo-nitzschia* in coastal ecosystems (Kelly et al. 2023; Sun et al. 2011; Trick et al. 2010; Xu et al. 2023), our understanding of the main environmental drivers influencing the geographic distribution of toxic *Pseudo-nitzschia* remains limited, preventing us from accurately forecasting their spatial distribution under future global change. We explored the oceanic distribution of toxic *Pseudo-nitzschia* along Chinese coasts and the Southern Ocean using historical data and our field surveys. To identify environmental drivers of toxic *Pseudo-nitzschia* abundance at a global scale, we analyzed meta-omics datasets from *Tara* Oceans and the Southern Ocean (our field survey project Southern Ocean Phytoplankton in a Changing Climate (SOPICC) from 2021 to 2023) using correlation analysis. Furthermore, we isolated the model toxic diatom *P. multiseries* from the Yellow Sea of China and maintained cultures for more than 2 years across a range of temperatures (5°C, 10°C, 15°C, 20°C, 25°C, and 30°C). Leveraging results from these laboratory simulation experiments, we conducted a logistical model to predict the growth and DA production of *P. multiseries* under the SSP2-4.5 climate condition from the Coupled Model Intercomparison Project Phase 6 (CMIP6) models (Eyring et al. 2016). This study thus addresses two fundamental questions: (1) What are the main environmental drivers for the global geographic distribution of toxic *Pseudo-nitzschia*? and (2) How will toxic *Pseudo-nitzschia* respond to current and future global climate change?

2 | Methods

2.1 | Meta-Omics Analysis of Global Distribution of Toxic *Pseudo-nitzschia*

To obtain a comprehensive understanding of the biogeographical distribution of *Pseudo-nitzschia* (at the genus level) and the four model toxic species—*P. multiseries*, *Pseudo-nitzschia multistriata*, *Pseudo-nitzschia delicatissima*, and *Pseudo-nitzschia pungens* (at the species level)—as well as the processes governing abundance and gene expression, we utilized metabarcoding (MetaB), metagenomic (MetaG), and metatranscriptomic (MetaT) datasets from *Tara* Oceans samples and field survey samples in the Southern Ocean. Meta-omics data from *Tara* Oceans are available at the European Nucleotide Archive under the project identifier PRJEB402. To supplement the omic datasets from *Tara* Oceans samples in the Southern Ocean, we conducted the field survey project Southern Ocean Phytoplankton in a Changing Climate (SOPICC) from 2021 to 2023. All phytoplankton samples from subsurface seawater (5 m) were collected using a submerged pump and removed large plankton by prefiltering through a 2000 μm filter membrane. Then, 1000, 4000, and 4000 mL filtered samples were passed through 0.22 μm polycarbonate membranes (Millipore, USA) in triplicate, stored at −80°C, and used for MetaB, MetaG, and MetaT analysis. The data of MetaB, MetaG, and MetaT have been deposited in the Sequence Read Archive (SRA) at the National Center for Biotechnology Information (NCBI) and are accessible through accession numbers PRJNA1286142, PRJNA1286158, and PRJNA1286141.

MetaB survey was based on the hypervariable V4 region of the 18S ribosomal RNA gene. 18S rRNA gene sequence data were

processed using a custom script with the QIIME software suite (Masella et al. 2012). First, forward and reverse reads were merged using FLASH (Magoč and Salzberg 2011). Following the merging of paired-end reads, sequences with a mean quality score > 20 were retained using fastp v0.20 (Chen 2023). Potential chimeric sequences were identified and removed using VSEARCH v1.11.1 (Edgar 2013). Next, quality-checked sequence reads were clustered into operational taxonomic units (OTUs) using DADA2 (Callahan et al. 2016). Finally, all OTUs were classified to the lowest possible taxonomic rank using the QIIME2 vsearch plugin based on the SILVA v138 database, using default parameters. OTUs represented by fewer than two sequence reads or without taxonomic assignment were discarded. Percentile normalization was applied to correct for batch effects in microbiome studies. The abundance of the *Pseudo-nitzschia* genus was extracted from the Meta B datasets and normalized to the barcode abundance of eukaryotic phytoplankton.

All metagenomic sequences were generated for 562 samples during the *Tara* Oceans expedition and were accessed from the European Molecular Biology Laboratory-European Bioinformatics Institute (EMBL-EBI). The raw reads were trimmed for quality using Fastp (v0.23.4) (Chen 2023). The clean data obtained from this process were used for subsequent analysis. To classify the largest possible number of algae species, all 278 algal reference genomes were obtained from the RefSeq database, and an algal library was constructed from these genomes. We constructed a custom Kraken2 (Lu et al. 2017) database incorporating standard reference genomes (including bacteria, archaea, viruses, protists, fungi, and plants) along with specialized algal genomic libraries (including Bacillariophyta, Charophyceae, Chlorophyta, Chrysophyceae, Cryptophyceae, Dinophyceae, Euglenozoa, Glaucocystophyceae, Phaeophyceae, Rhodophyta, Xanthophyceae). Finally, all clean reads were taxonomically classified using Kraken2 based on the custom database, and species-level abundance was estimated with Bracken. The abundance of microbial sequence read counts was normalized for each taxonomic group to account for varying sequencing depths across samples. The abundance information for *P. multiseries*, *P. multistriata*, *P. delicatissima*, and *P. pungens* was extracted from the MetaG datasets and compared with all eukaryotic phytoplankton. The relative strength of significant environmental variables in explaining the bioabundance was analyzed by generalized additive models (GAMs) (Hastie 2017).

We used metatranscriptomics data to estimate gene transcript detection associated with the domoic acid biosynthetic pathways in *Tara* Oceans samples. First, the UniGene catalog sequence from *Tara* Oceans samples was downloaded from EMBL-EBI. Genes related to domoic acid biosynthesis, *dabA*, *dabB*, *dabC*, *dabD*, and *slc6*, were extracted from the whole genome of *P. multiseries*, *P. multistriata*, *P. delicatissima*, and *P. pungens*. To calculate fragments per kilobase per million mapped reads (FPKM), the number of fragments aligned to a transcript is first divided by the transcript length in kilobases to normalize for gene length, then divided by the total number of mapped fragments (in millions) to account for sequencing depth. This metric is primarily used for intrasample gene expression comparisons

in eukaryotic organisms. For quantification, we used the hisat2 (v2.2.1) software to align the clean data of *Tara* Oceans to the reference genes and stringtie (v2.2.1) software to calculate the FPKM value.

We correlated the abundance of the *Pseudo-nitzschia* genus and four toxic species—*P. multiseries*, *P. multistriata*, *P. delicatissima*, and *P. pungens* with—environmental data collected during the *Tara* Oceans expeditions. Contextual environmental data, including sea surface temperature (SST), pCO_2, salinity, Chlorophyll a (Chla), nitrate (NO_3^-), phosphate (PO_4^{3-}), and silicate (SiO_3^{2-}), were inferred for the surface layer of the sampling station. We complemented these measurements with (i) SST, SSS, NO_3^-, PO_4^{3-}, and SiO_3^{2-} from the World Ocean Atlas 2013 (WOA13) database (Garcia et al. 2013), (ii) Chla concentration and pCO_2 data extracted from CMIP6 (Eyring et al. 2016). If data were unavailable for the latitude and longitude coordinates of the sample, mean values of a 2° square around the sampling location were used.

2.2 | Data Search, Cruise Survey, and Sampling of *Pseudo-nitzschia* Along Chinese Coasts

We carried out a systematic literature review in China National Knowledge Infrastructure (CNKI), Web of Science, and Google Scholar to identify all data documenting the geographic distribution or algal abundance of *Pseudo-nitzschia* along the Chinese coasts from 1997 to 2023 (Supporting Information S2, Figure S1). To investigate the effect of environmental factors on the spatial and temporal dynamics of *Pseudo-nitzschia* abundance in natural phytoplankton communities among different oceans along Chinese coasts, we conducted cruise surveys in Spring (April 12–27), Summer (July 12–29), and Autumn (October 19–November 4) in the Bohai and Yellow Seas in 2022. We collected surface seawater samples from a depth of 2.0 m using a submerged pump and removed large plankton by prefiltering through a 2000 μm filter membrane. A 1000 mL filtered sample was fixed with 2% buffered formalin and stored in darkness for further microscopic observation. Due to the difficulty of visually identifying *Pseudo-nitzschia* at the species level by microscopic observation, the morphologically based abundance (MorP) of *Pseudo-nitzschia* was identified at the genus level and enumerated under an inverted Nikon Eclipse Ti-U microscope (Nikon, Tokyo, Japan) at magnifications of 400–600× with a known volume (0.1 mL) of fixed water samples. Additional filtered samples (1000 and 4000 mL) were passed through 0.45 μm polycarbonate membranes (Millipore, USA), stored at −80°C, and used for metabarcoding (MetaB) and metagenomic (MetaG) analysis, the data of which have been deposited in SRA at the NCBI and are accessible through accession number PRJNA1286164 and PRJNA1286163.

The MetaB-based abundance of the *Pseudo-nitzschia* genus was normalized to eukaryotic phytoplankton. We also calculate the relative abundance of four toxic species—*P. multiseries*, *P. multistriata*, *P. delicatissima*, and *P. pungens* relative—to eukaryotic phytoplankton based on metagenomic sequencing using Kraken2 classifier (Lu et al. 2017). Moreover, to analyze *Pseudo-nitzschia* community composition, we used all sequences of

Pseudo-nitzschia species in Genbank, including nuclear ribosomal RNA (18S, 28S, ITS1-5.8S-ITS2), chloroplast and mitochondrial genes, complete organelle genome sequences, as well as transcriptome and whole genome sequences as reference dataset to annotate *Pseudo-nitzschia* species sequences from metagenomic data.

At sampling stations, we monitored annual changes in SST, salinity, pH, and Chlorophyll a (Chla) using a conductivity–temperature–depth recorder (CTD SBE-911 plus, Sea Bird Electronics Inc., USA) and a Multiparameter Sonde YSI 6600. We collected and filtered 100 mL seawater through 0.45 μm polycarbonate membranes (Millipore, USA) and determined the nutrient concentration of total dissolved inorganic nitrogen (DIN), phosphorus (PO_4^{3-}), and silicate (SiO_3^{2-}) using an AutoAnalyzer (BRAN and LUEBBE AA3, Germany). We then conducted analyses with GAMs to assess the relative strength of significant environmental variables in explaining the morphological-based abundance (MorP), MetaB-based abundance, or MetaG-based abundance of various *Pseudo-nitzschia* species.

2.3 | Laboratory Experiment to Study Physiological Responses of *P. multiseries* to Ocean Warming

As the most abundant among the four toxic *Pseudo-nitzschia* species at the global level, we studied the evolutionary responses of *P. multiseries* to ocean warming. Algal cultures were maintained under semi-continuous culture conditions at six temperature levels (5°C, 10°C, 15°C, 20°C, 25°C, and 30°C) in a programmed chamber (HP1000G-D, China) to achieve the desired temperature treatments. The low and high temperatures of 5°C and 30°C were chosen to coincide with the lower and upper thermal tolerance limits for *P. multiseries*. Pilot experiments revealed that growth almost ceased below 5°C or above 30°C, while the selected experimental temperatures were within the environmental range for this widely distributed species. Triplicate populations were maintained in 800 mL of adjusted f/2 medium (with 100 μm NO_3^-, 6 μm PO_4^{3-}, and 100 μm SiO_3^{2-}) in 1000 mL Schott Duran flasks for each selection regime ($6 \times 3 = 18$ cultures). The standard culture condition at 20°C was defined as the control. The selection temperatures at 5°C, 10°C, 15°C, 20°C, 25°C, and 30°C were gradually adjusted by 1°C per day. The selection experiment lasted for 800 days (160 batch cycles), with the corresponding generations ranging from 249 ± 3.1 to 621 ± 3.1 in different selection groups (Table S1). During the acclimation phase, 2×10^4 cells were transferred into fresh medium every 5 days to initiate the next batch cycle. The algal specific growth rate (SGR, day^{-1}), particulate organic carbon (POC), particulate DA (pDA) and dissolved DA (dDA) were determined on the fourth day of each batch cycle. The DA production rate (y, expressed as [μg C^{-1} day^{-1}]) was calculated as follows:

$$y = e^{\mu} \times c \tag{1}$$

where μ is the specific growth rate (SGR, day^{-1}) and c is DA concentration (the sum of the pDA and dDA, μg C^{-1}). The average values of these traits across 20 days (four batch cycles) were calculated and presented as the evolutionary responses to different selection treatments.

2.4 | DA Determination

Based on the MorP-based or MetaB-based biogeography of *Pseudo-nitzschia* in the Bohai and Yellow Seas of China, 171 samples were collected in triplicate for DA determination in dissolved seawater (dDA), suspended particulate matter (SPM), and phytoplankton. We filtered 2000 mL seawater using a 0.7 μm glass microfiber (GF/F, Whatman) to separate the dDA and SPM, which were stored at −20°C in the dark. An additional 500 L of seawater was pumped and filtered through a 20 μm pore size net, condensed to 500 mL, and subsequently filtered through 1.6 μm GF/A filters (Whatman), then stored at −20°C until DA analysis. DA determination in dDA, SPM, and phytoplankton was conducted using liquid chromatography-high resolution mass spectrometry and liquid chromatography–tandem mass spectrometry (an online SPE-LC–MS/MS system) following the method described by Wang et al. (2021). However, we found that DA was predominantly in a dissolved phase (> 99.5%) in seawater, and DA levels in SPM and phytoplankton were consistently below the limit of detection (LOD) (Figure S2). As a result, only the dDA results are presented in our study. In the laboratory selection experiment, algal cellular DA was extracted using 10% methanol/water (8 mL methanol: water, 1:9, v/v) according to the method of Wang et al. (2012) with minor modifications. Whatman GF/F glass fiber filters (0.45 μm, 25 mm diameter, Whatman, Germany) were used to collect cells and filtrate from the cultures to determine cellular and dissolved DA. The LC–MS/MS method was used to determine DA at the Key Laboratory of Testing and Evaluation for Aquatic Product Safety and Quality, Ministry of Agriculture and Rural Affairs, P. R. China (Qingdao). LC–MS/MS analysis was performed using a U3000 HPLC system (Thermo Scientific, USA) coupled to a Thermo TSQ Endura mass spectrometer equipped with an ESI source operated in positive ionization mode.

2.5 | Illustrative Global Models

To illustrate the global distribution map and changes in the abundance and DA production rates of toxic *P. multiseries* under the SSP2-4.5 climate scenario, we used and compared two modeling approaches in the present study. First, we applied a machine learning method, the generalized additive model (GAM), to generate global maps using MetaG datasets from *Tara* Oceans and key environmental factors, including only significant drivers of algal abundance ($p < 0.05$) across different size fractions in the model. Second, to depict the spatial and temporal dynamics of *P. multiseries* in response to ocean warming, we used a data-derived statistical model relating SGR and DA production rate to temperature from the laboratory experiment. Projected changes through the 21st century were modeled using outputs from CMIP6 (Eyring et al. 2016), under the SSP2-4.5 scenario of SST. Based on data from laboratory selection experiments, response curves of growth rates and DA production rates to different temperatures were estimated as the best-fit polynomial formulae. Since DA production rate varied significantly across experimental temperature ranges, we log-normalized DA production rate (LgDA production rate). We modeled the changes in specific growth rate (ΔSGR) and Lg (DA production rate)

(ΔLgDA) as the difference between 2015 and 2100 on a global map. Temporal variation in SGR and Lg (DA production rate) was modeled using the mean SST from four global climate models from CMIP6 for the periods 2010–2100.

3 | Results

3.1 | Global Distribution of Four Toxic *Pseudo-nitzschia* Species and Potential Environmental Drivers

We investigated the global distribution patterns of four toxic *P. multiseries*, *P. multistriata*, *P. delicatissima*, and *P. pungens*—along with *Pseudo-nitzschia* community composition (Figure 1, Figures S3–S5), using meta-omics datasets from the *Tara* Oceans project and field surveys conducted during the Southern Ocean Phytoplankton in a Changing Climate (SOPICC) expedition from 2021 to 2023. We found that these species are widely distributed from pole to pole and across coastal to open ocean environments, spanning a broad temperature range from −1.81°C to 31.2°C (Figure 1, Figures S3 and S4). Among the four species, *P. multiseries* exhibits the highest relative abundance (Figure 1a), being 3.03, 1.06, and 1.02 times greater than *P. multistriata* (Figure 1b), *P. delicatissima* (Figure 1c), and *P. pungens* (Figure 1d), respectively.

We found evidence of species-specific distribution patterns at the global scale, along with species-specific responses to environmental variables. Comparing polar and nonpolar ecosystems, the four toxic species—*P. multiseries*, *P. multistriata*, *P. delicatissima*, and *P. pungens*—show notably higher abundances in the Southern Ocean (SO) than in the Arctic Ocean (AO) and nonpolar oceans. Due to differences in survey years and methodologies among the datasets, we categorized samples broadly as either polar or nonpolar when analyzing correlations between species abundance and environmental variables. In nonpolar oceans, SST shows a significant positive correlation with the abundance of *P. multiseries* ($p < 0.001$ for 0.8–5 μm size fraction and $p < 0.01$ for 0.8–2000 μm size fraction), *P. multistriata* ($p < 0.05$ for 0.8–5 μm size fraction, $p < 0.001$ for 20–180 μm size fraction, and $p < 0.001$ for 180–2000 μm size fraction), and *P. pungens* ($p < 0.05$ for 0.8–5 μm size fraction), but no significant effect on *P. delicatissima* ($p > 0.05$ for all size fractions). By contrast, in polar oceans, SST does not show a significant correlation with algal abundance, either in the Arctic Ocean (AO) (Figure S3) or the Southern Ocean (SO) (Figure S4).

To further explore toxin contamination in natural ocean environments, we analyzed DA biosynthesis gene expression across the global ocean using metatranscriptome datasets from *Tara* Oceans (Figure 2). Our analysis revealed discrepancies between species abundance and the expression of core genes involved in the DA metabolic pathway on a global scale (Figures 1 and 2). We found that *slc6* exhibited a broader regional transcript detection compared to *dabA*, *dabB*, *dabC*, and *dabD*. For example, the *dabB* transcript was only detected in *P. multistriata* at one station in the Northwest Atlantic (NWA, *Tara*145). The *dabA* transcript was detected in *P. multiseries* at two stations in the Southwest Atlantic (SWA, *Tara*80) and Southeast Pacific (SEPC, *Tara*92), and in *P. multistriata* at three stations in the Mediterranean–East Pacific Convergence (MEPC, *Tara*135), NWA (*Tara*145),

and AO (*Tara*205). The *dabC* transcript was detected in *P. multiseries* at three stations in the Middle East Pacific (MEP, *Tara*123) and AO (*Tara*188 and *Tara*205), and in *P. multistriata* at one station in NWA (*Tara*145). The *dabD* transcript was detected in *P. multiseries* at one station in AO (*Tara*188), in *P. multistriata* at three stations in NWA (*Tara*145) and Eastern Atlantic (EA, *Tara*65 and *Tara*151), in *P. delicatissima* at three stations in SWA (*Tara*80) and AO (*Tara*196 and *Tara*206), and in *P. pungens* at one station in SEPC (*Tara*92). By contrast, the *slc6* transcript was widely detected in *P. multiseries*, *P. multistriata*, and *P. delicatissima* at 12 stations in MEP, NWA, SWA, EA, AO, and SO.

3.2 | Seasonal Patterns in DA Contamination and *Pseudo-nitzschia* Distribution Along the Chinese Coast

We determined the spatial and temporal variation of DA concentrations dissolved in dDA, SPM, and phytoplankton in the Bohai and Yellow Seas of China (Figure 3a, Figure S2). We found that the detection rate of DA in SPM (9%) and phytoplankton (3%) was significantly lower than in dDA (99%) indicating that DA in the environment was primarily preserved in the dissolved phase. dDA exhibited a clear seasonal variation pattern, being highest in summer (ranging from 0.8 to 16.2 ng L⁻¹, mean: 3.3 ± 0.4 ng L⁻¹), intermediate in autumn (ranging from 0.7 to 12.7 ng L⁻¹, mean: 3.1 ± 0.3 ng L⁻¹), and lowest in spring (ranging from 0.3 to 1.6 ng L⁻¹, mean: 0.6 ± 0.1 ng L⁻), with the mean sampling temperature at 24.9°C ± 1.6°C, 17.5°C ± 0.8°C, and 9.8°C ± 2.0°C, respectively (Figure 3a). Variation in dDA (ranging from 0.3 to 16.2 ng L⁻¹) was driven by temperature ($F = 33.81$, $p < 0.001$) and pH ($F = 6.44$, $p < 0.001$, Figure 3b). Moreover, temperature was the most important environmental factor for its spatial and temporal variation, accounting for 66.7% of the total explained variances.

To further determine the regional distribution of toxic *Pseudo-nitzschia*, we collected and analyzed the relative abundance of *Pseudo-nitzschia* within eukaryotic phytoplankton communities on interannual timescales in the Bohai and Yellow Seas using Morp, MetaB, and MetaG data. Based on morphological counting, algal abundance was highest in summer (319.7 ± 1016.6 cells L⁻¹), compared to autumn (122.7 ± 198.5 cells L⁻¹) and spring (14.2 ± 17.2 cells L⁻¹) (Figure 4a). Consistent with morphological data, the highest *Pseudo-nitzschia* abundance based on metabarcoding data was also observed in summer (Figure 4b). However, the relative abundance of *Pseudo-nitzschia* based on metabarcoding data in spring was higher than in autumn.

Based on the four publicly available sets of *Pseudo-nitzschia* genome and metagenomic data, we found that all four bloom-forming toxic species (*P. multiseries*, *P. multistriata*, *P. delicatissima*, and *P. pungens*) were simultaneously distributed along the Chinese coast (Figure 4c). Furthermore, metagenomic sequencing indicates that the species composition of the *Pseudo-nitzschia* community was more complex than expected, with 25 toxic *Pseudo-nitzschia* species and 27 nontoxic species detected (Figure S6a). Consistent with the morphological data, the highest algal abundances of *P. delicatissima* ($F = 6575.86$, $p < 0.001$) based on MetaG were observed in the warmer summer months and the lowest in the colder spring months. However, the highest abundances of *P. multiseries*
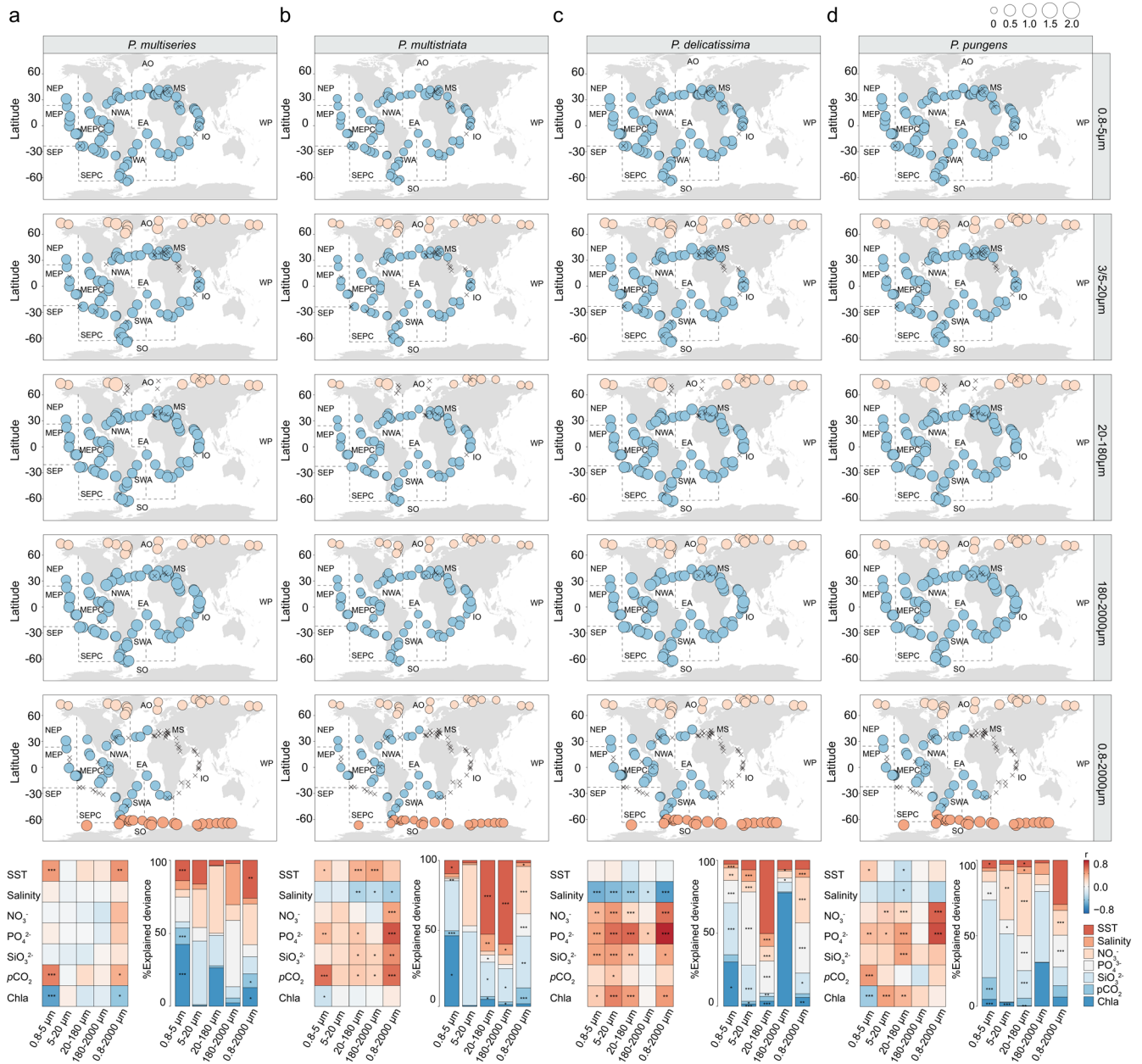
FIGURE 1 | Geographic distribution of four toxic *Pseudo-nitzschia* species across the global ocean based on MetaG datasets from polar and non-polar oceans and potential environmental drivers. Global distribution of toxic *P. multiseries* (a), *P. multistriata* (b), *P. delicatissima* (c), and *P. pungens* (d) and correlation of contextual variables with their abundances. The blue, light red and deep red bubbles represent samples in nonpolar oceans, Arctic Ocean, and Southern Ocean, respectively. The bubble size varies according to the abundance gradient, while crosses indicate absence. The color of the tiles indicates the correlation coefficient and asterisks represent the statistical significance (*** $p < 0.001$, ** $p < 0.01$, * $p < 0.05$). The individual explained deviance and additive contribution of the seven main contextual variables normalized to the total explained deviance in GAMs. The abbreviations of NEP, MEP, SEP, MEPC, SEPC, and WP represent Northern East Pacific, Middle East Pacific, Southern East Pacific, Middle East Pacific Coast, Southern East Pacific Coast, and Western Pacific; NWA, SWA, and EA represent Northern West Atlantic, Southern West Atlantic, and Eastern Atlantic; AO, SO, and IO represent Arctic Ocean, Southern Ocean, and Indian Ocean; MS represents Mediterranean Sea. Map lines delineate study areas and do not necessarily depict accepted national boundaries.

($F = 21.34$, $p < 0.001$), *P. multistriata* ($F = 329.85$, $p < 0.001$), and *P. pungens* ($F = 101.75$, $p < 0.001$) were observed in the relatively cooler autumn months, suggesting species-specific optimum growth temperatures (Figure 4d,e).

SST emerged as the most dominant environmental predictor, accounting for 47.8%, 32.3%, 47.5%, and 47.4% of the

total explained variance for MorP-based abundance, MetaB-based abundance, MetaG-based *P. multiseries* abundance, and MetaG-based *P. delicatissima* abundance, respectively (Figure 4d,e). To identify environmental drivers of *Pseudo-nitzschia* distribution, we conducted a correlation analysis between algal abundance and field measurements of physical parameters (SST and salinity), chemical parameters (total
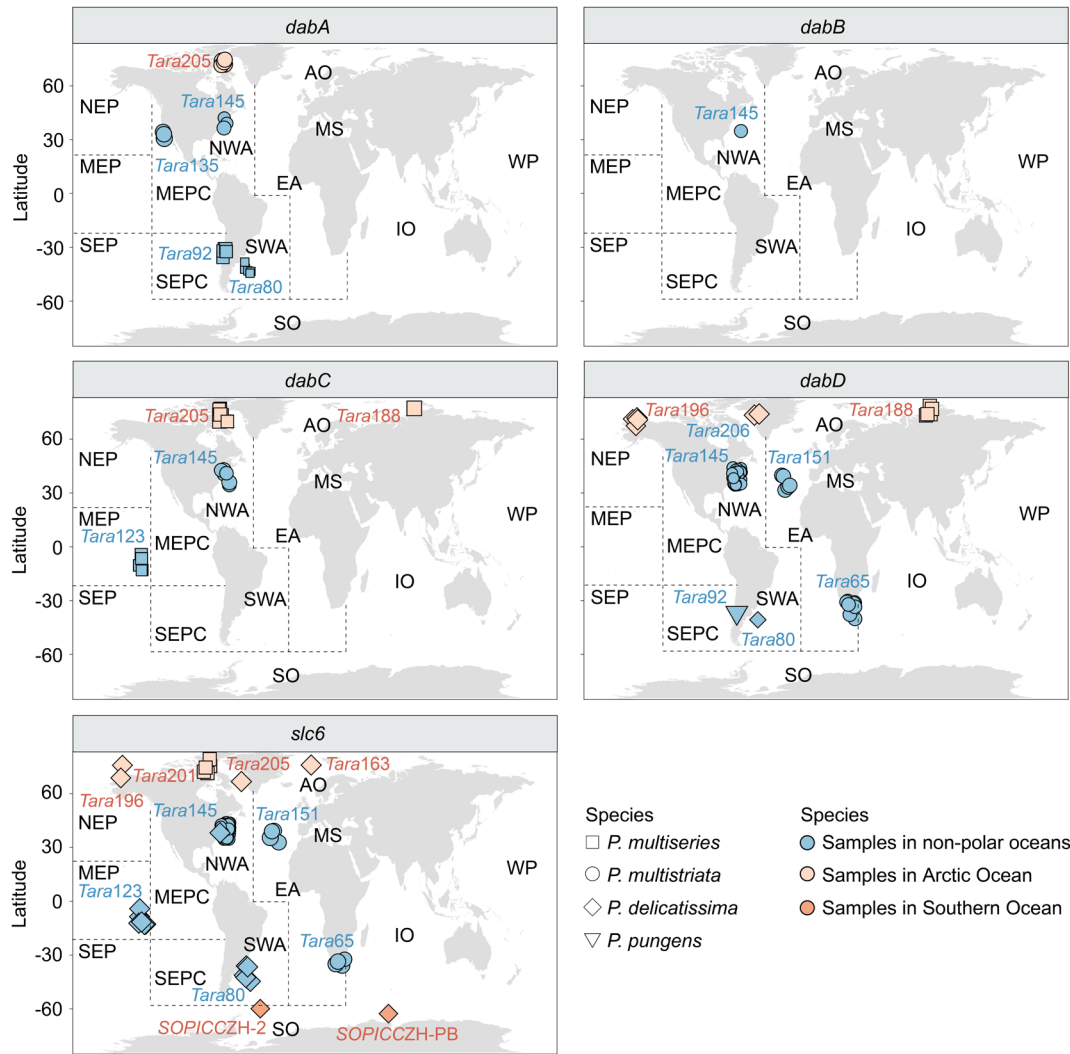
FIGURE 2 | Relative expression of core genes involved in the DA metabolic pathway of toxic *P. multiseries*, *P. multistriata*, *P. delicatissima*, and *P. pungens* using metatranscriptomics datasets from *Tara* Oceans and field survey project Southern Ocean Phytoplankton in a Changing Climate (SOPICC). The five core genes involved in DA metabolic pathway include *dabA*, *dabB*, *dabC*, *dabD*, and *slc6*. The abbreviations of NEP, MEP, SEP, MEPC, SEPC, and WP represent Northern East Pacific, Middle East Pacific, Southern East Pacific, Middle East Pacific Coast, Southern East Pacific Coast, and Western Pacific; NWA, SWA, and EA represent Northern West Atlantic, Southern West Atlantic, and Eastern Atlantic; AO, SO, and IO represent Arctic Ocean, Southern Ocean, and Indian Ocean; MS represents Mediterranean Sea. Map lines delineate study areas and do not necessarily depict accepted national boundaries.

dissolved inorganic nitrogen concentration (DIN), PO_4^{3-}, SiO_3^{2-}, and pH), and a proxy for the trophic status of the system (Chlorophyll a, Chl a). We found that SST ($F = 24.27$, $p < 0.01$), pH ($F = 2.02$, $p < 0.05$), PO_4^{3-} ($F = 3.92$, $p < 0.001$), and SiO_3^{2-} ($F = 13.85$, $p < 0.05$) all showed significant positive effects on MorP-based abundance, whereas SST ($F = 10.16$, $p < 0.01$) and PO_4^{3-} ($F = 10.18$, $p < 0.05$) showed significant positive effects on MetaB-based abundance (Figure 4d). At the species level, SST ($F = 15.69$, $p < 0.01$), salinity ($F = 0.07$, $p < 0.01$), PO_4^{3-} ($F = 12.19$, $p < 0.05$), and SiO_3^{2-} ($F = 2.79$, $p < 0.01$) showed significant effects on MetaG-based *P. multistriata* abundance; DIN ($F = 3.45$, $p < 0.05$) and pH ($F = 10.72$, $p < 0.01$) showed significant effects on MetaG-based *P. multiseries* abundance; SST ($F = 4.20$, $p < 0.001$) and Chl a ($F = 3.59$, $p < 0.01$) showed significant effects on MetaG-based *P. delicatissima* abundance, and salinity ($F = 9.56$, $p < 0.01$) showed significant effects on MetaG-based *P. pungens* abundance.

3.3 | Modelling Projections of Toxic *P. multiseries* Dynamics and DA Production Under Further Climate Change

We used two modeling approaches to project changes in the abundance and DA production rate of the most globally abundant toxic *Pseudo-nitzschia* species, *P. multiseries*, under the SSP2-4.5 climate scenario (Figure 5). We found that although *P. multiseries* abundance decreased in the tropical Western Pacific and tropical Atlantic, it increased by 31.2% in the 0.8–5 μm size fraction (Figure 5a) and 75.4% in the 0.8–2000 μm size fraction (Figure 5b) at the global scale by the end of the century under the SSP2-4.5 climate scenario.

To assess long-term temperature effects on *P. multiseries* physiology, we conducted an experimental evolution study using isolates from southeast Sungo Bay in the Yellow Sea,
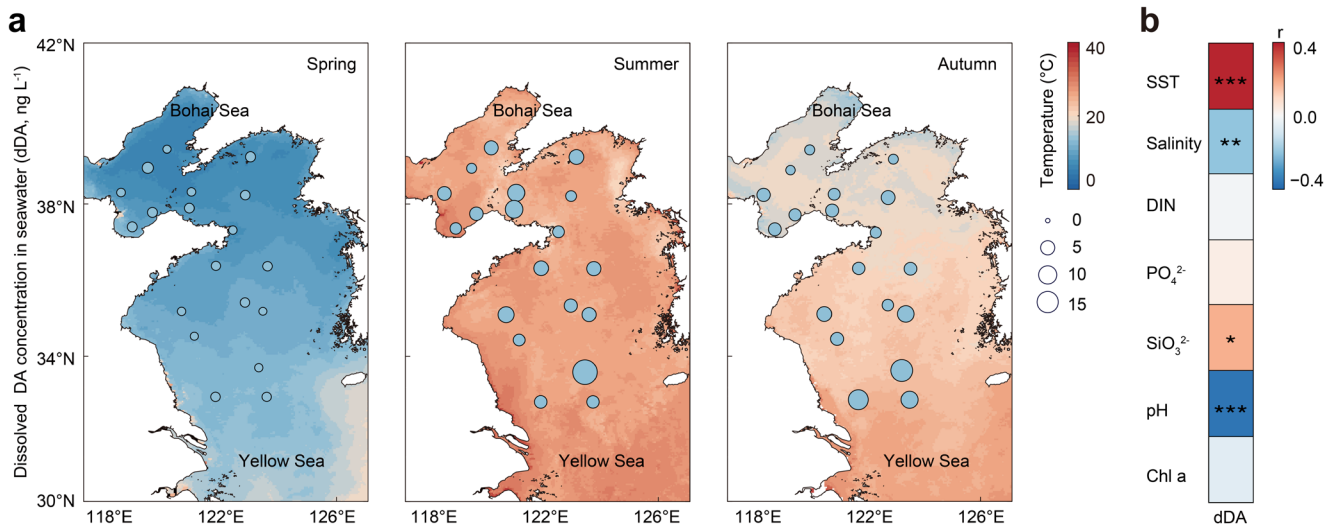
FIGURE 3 | Spatial and temporal variation of DA contamination in natural seawater along the Chinese coast. (a) Variations in dissolved DA concentration (dDA) in natural seawater among different sampling seasons. (b) Correlation of contextual variables with dDA. The color of the tiles indicates the correlation coefficient and asterisks represent statistical significance (***$p < 0.001$, **$p < 0.01$, *$p < 0.05$). Map lines delineate study areas and do not necessarily depict accepted national boundaries.

China (37°02′N, 122°33′E). Cultures were maintained at 5°C, 10°C, 15°C, 20°C, 25°C, and 30°C for approximately 800 days (Figure S7). Consistent with the observed effect of SST on *P. multiseries* distribution in the Chinese coastal and global oceans, our results revealed significant shifts in specific growth rate (SGR) and DA production (Figure S7a; $F = 714.7$, $p < 0.0001$ and Figure S7b; $F = 17,204$, $p < 0.0001$). *P. multiseries* SGR peaked at 20°C, while DA production spiked at 30°C.

Projecting these findings under future warming, we utilized statistical relationships to forecast growth and DA production under the SSP2-4.5 scenario. Our global model projections showed that the absolute magnitude of changes in SGR (Figure 5c) and DA production rate (ΔlgDA, the change in the log of DA production rate, Figure 5d) varied across different climatic zones in the global ocean. The SGR generally decreased in tropical oceans but increased in subtropical, temperate, and high-latitude oceans (Figure 5c). This trend mirrored the generalized additive model (GAM)-based algal abundance changes (Figure 5a). Conversely, DA production rates are expected to increase globally, with the sharpest increases in tropical and temperate waters (Figure 5d). By 2100, under SSP2-4.5, SGR may experience a modest 0.5% increase (Figure 5e). In contrast, our model predicts significant DA production increases of up to 200.4% by the end of this century (Figure 5f), relative to present levels.

4 | Discussion

4.1 | Widespread Distribution of Toxic *Pseudo-nitzschia* Across Coastal and Oceanic Waters

With increasing discovery and reporting of new *Pseudo-nitzschia* species, the known global distribution of this genus has expanded significantly (Bates et al. 2018; Jabre et al. 2021; Zhu et al. 2017). Our results offer a unique and comprehensive perspective on the global distributions of four of the model

toxic *Pseudo-nitzschia* species using field survey data along the Chinese coasts and from the Southern Ocean Phytoplankton in a Changing Climate (SOPICC) project (the first systematic survey around the Antarctic Circle from 2021 to 2023), coupled with global meta-omics data from the *Tara* Oceans survey (Figure 1). Although previously they have been considered largely from a local coastal bloom perspective (Bates et al. 2018; Silver et al. 2010; Zhu et al. 2017), our results demonstrate that these four toxic species are, in fact, abundant worldwide in both coastal and open oceanic ecosystems and are present from pole to pole. This underscores the fact that toxic *Pseudo-nitzschia* are not confined to coastal upwelling zones or temperate shelves but are instead a pervasive component of phytoplankton communities throughout the global ocean.

Several studies have highlighted regional differences in species composition and potential environmental drivers (Bowers et al. 2018; Chen et al. 2023; Clark et al. 2019; Lundholm et al. 2010; Radan and Cochlan 2018). However, through metagenomic sequencing and marker gene blasting, we found that 22 toxic *Pseudo-nitzschia* species co-occurred globally (Figure S6). This evidence underscores the need to expand biological monitoring capacities and sampling methods to obtain more comprehensive information on the global distribution of toxic *Pseudo-nitzschia* species (Bowers et al. 2018). Thus, virtually the entire ocean is at potential risk if climate change drives an increase in *Pseudo-nitzschia* growth and toxicity.

4.2 | Molecular Forecasting of Domoic Acid Contamination Risk

Five key genes—*dabA*, *dabB*, *dabC*, *dabD*, and *slc6* are—implicated in the DA biosynthesis and transport pathway (Brunson et al. 2018; Boissonneault et al. 2013). Notably, only the highly toxic *P. australis* has been reported to express the *dab* genes in natural environments (Brunson et al. 2018). Recently, Brunson et al. (2024) reported that the co-expression of the *dabA* and *sit1*

FIGURE 4 | Legend on next page.

genes could serve as a robust predictor of DA 1 week in advance of toxicity, potentially enabling the forecasting of DA-producing HABs. By contrast, we found that the *slc6* transcript was widely detected in *P. multiseries*, *P. multistriata*, and *P. delicatissima* at 12 stations of *Tara* Oceans in MEP, NWA, SWA, EA, AO, and SO (Figure 2), regions where toxic *Pseudo-nitzschia* species have been

FIGURE 4 | Biogeography and environmental drivers of *Pseudo-nitzschia* in the Bohai and Yellow Seas of China. (a) Biogeography and cell abundance of *Pseudo-nitzschia* based on morphological data (MorP). The blue bubble size varies according to the abundance gradient (log-normalized cell concentration), while crosses indicate absence. (b) Biogeography and algal abundance of *Pseudo-nitzschia* based on metabarcoding data (MetaB). (c) Biogeography and algal abundance of toxic *P. multiseries*, *P. multistriata*, *P. delicatissima*, and *P. pungens* based on MetaG datasets. (d) Correlation of contextual variables with algal abundance based on MorP, MetaB, and MetaG. The color of the tiles indicates the correlation coefficient and asterisks represent statistical significance (***$p < 0.001$, **$p < 0.01$, *$p < 0.05$). (e) The individual explained deviance and additive contributions of the four main contextual variables normalized to the total explained deviance in GAMs. Map lines delineate study areas and do not necessarily depict accepted national boundaries.
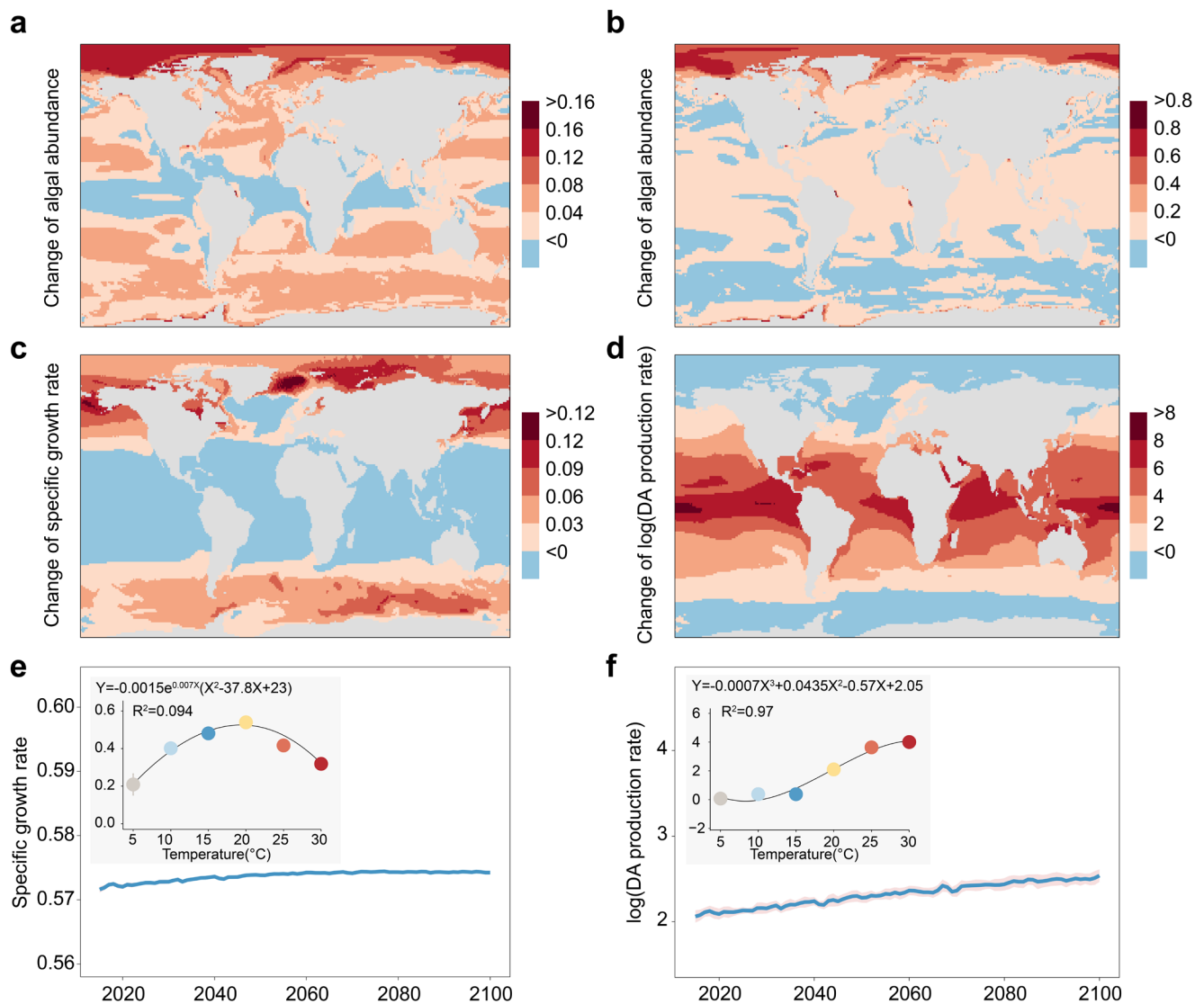
FIGURE 5 | Global model projections of changes in abundance and DA production rate of toxic *P. multiseries* under the SSP2-4.5 climate scenario based on MetaG datasets from *Tara* Oceans and 800-day laboratory culture experiments. Illustrative global models of changes in algal abundance of *P. multiseries* in the 0.8–5 μm size fraction (a) and in the 0.8–2000 μm size fraction (b) using a generalized additive model (GAM). Illustrative global models of changes in *P. multiseries* specific growth rate (SGR) (c) and DA production rate (log-normalized DA) (d) based on the statistical relationships between SGR or DA production rate and temperature from a long-term acclimation experiment of 800 days. Time series of *P. multiseries* SGR (e) and DA production rate (f) from present day to the end of the century. Map lines delineate study areas and do not necessarily depict accepted national boundaries.

shown to produce DA (Bates et al. 2018). Since the SLC6 acts as the DA transporter from inside to outside the cell (Boissonneault et al. 2013), we propose that the gene expression of *slc6* be further investigated to determine its potential as a genetic marker for monitoring DA exposure risk in natural environments.

However, global gene expression in *Tara* Oceans exploration was not detected in the Indian Ocean or the Mediterranean Sea, despite the abundant distribution of the four toxic species in these areas. The evidence suggests that caution is needed when linking *Pseudo-nitzschia* abundance with DA contamination, as not all

strains produce the toxin, and those that do may do so intermittently (Bates et al. 2018). Moreover, phylogenetic analysis indicated that several core genes *dabA*, *dabC*, *dabD*, and *slc6* (Figure S8) involved in the DA metabolic pathway were not specific to *Pseudo-nitzschia*, but are widely detected in other species, such as red algae and bacteria. Therefore, further research is essential to clarify the functional specificity and expression dynamics of these genes in *Pseudo-nitzschia* and to establish more precise molecular tools for predicting DA contamination events in marine environments.

4.3 | Multi-Omics Integration Reveals DA Contamination Risk in Chinese Coastal Waters

Historical records show the widespread distribution of *Pseudo-nitzschia* along the Chinese coast over the past 30 years (see Supporting Information S2, Figure S1), but few DA records are available from natural communities due to limited monitoring and analysis. In this study, we integrated traditional morphological counting methods with meta-omics approaches for the first time to analyze the abundance and distribution of *Pseudo-nitzschia* in the Bohai and Yellow Seas of China (Figure 4). The inconsistency between MorP and MetaB in spring and autumn could be attributed to substantial variation in 18S rDNA copy number among phytoplankton species, which can range from one to more than 12,000 copies (Wang et al. 2022; Zhu et al. 2005) or to misidentification by microscopy or an incomplete rDNA reference database. Our field survey data confirm that multiple detection methods are necessary to assess the blooming potential of toxic *Pseudo-nitzschia* assemblages. Previous reports identified *P. simulans*, *P. fukuyoi*, *P. cuspidata*, *P. pseudodelicatissima*, *P. fraudulenta*, *P. multiseries*, and *P. lundholmiae* as the primary toxigenic species in Chinese coastal waters (Dong et al. 2020; Lü et al. 2012; McCabe et al. 2016; Huang et al. 2019). By contrast, our results based on metagenomic sequencing further indicated that 25 toxic *Pseudo-nitzschia* species and 27 nontoxic species were simultaneously detected in the Bohai and Yellow Seas of China (Figure S6a).

DA phase partitioning analysis further found that dDA dominated the DA pool in the Bohai and Yellow Seas (Figure 3), diverging from patterns in some temperate systems where particulate DA is more prevalent during *Pseudo-nitzschia* blooming (Delegrange et al. 2018; Schnetzer et al. 2007). However, previous studies also demonstrated that dDA is commonly released by toxic *Pseudo-nitzschia* (Sekula-Wood et al. 2009; Trainer et al. 2012). Therefore, establishing an integrated three-tier monitoring network encompassing the environment, seawater, phytoplankton, and seafood is essential for the early warning of domoic acid (DA) contamination risk.

4.4 | Sea Surface Temperature Drives *Pseudo-nitzschia* Distribution and DA Production

Environmental correlation analysis using both global data and regional data indicated that SST acts as the most dominant environmental driver for *Pseudo-nitzschia* distribution and DA production (Figures 1, 3, and 4). Numerous studies have reported the influence of changing temperature on various *Pseudo-nitzschia* species, although some found contradictory results

(Zhu et al. 2017; Kelly et al. 2023; Xu et al. 2023). Importantly, few studies have systematically examined the temperature-dependent dynamics of growth and DA production across the full range of environmental temperatures. Zhu et al. (2017) assessed the thermal responses of a *P. australis* isolate from Southern California across a temperature range from 12°C to 30°C and found that maximal growth rates occurred at 23°C (~0.8 day^{-1}). However, cellular DA concentration became detectable only at 23°C and increased to maximum levels at 30°C, despite a decrease in the specific growth rate (SGR) due to thermal inhibition (Zhu et al. 2017). These results demonstrated that cellular toxicity was directly influenced by temperature, rather than being an indirect function of growth rate. Compared with *P. australis*, the *P. multiseries* isolate from the Yellow Sea, China, could grow across a broader temperature range from 5°C to 30°C, exhibiting a similar maximum growth rate at 20°C and the highest DA production at the highest temperature of 30°C (Figure S7). This broad growth temperature range aligns with its cosmopolitan distribution and higher abundance across tropical, temperate, and polar ecosystems (Bates et al. 2018).

The importance of temperature for *Pseudo-nitzschia* distributions is supported by previous studies showing that increasing ocean temperatures are expected to modify the seasonal changes in phytoplankton diversity and alter the supply of nutrients to surface waters (Chen et al. 2023; Ibarbalz et al. 2019; Kling et al. 2020). Given the role of nutrient conditions, many studies have shown that the dynamics of *Pseudo-nitzschia* blooms and DA production are consistently correlated with nitrogen or silicate sources in coastal ecosystems such as in Chesapeake Bay, the Southern North Sea, the Sea of Marmara, and Mariager Fjord (Delegrange et al. 2018; Lundholm et al. 2010). A few studies found that phosphate concentration and Si/N/P ratios influence *Pseudo-nitzschia* growth and DA production, such as during blooms in the Southern California Bight (Trainer et al. 2012). Our study found that phosphate concentration was more important than nitrogen concentration in driving changes in *Pseudo-nitzschia* abundance along the Chinese coasts (Figure 4d). This could be due to phosphorus limitation in the sampling seawater, as no significant differences were found in nitrogen and silicate availability between sampling stations (Moon et al. 2021).

5 | Conclusions

Our findings confirm that temperature is a key driver of domoic acid (DA) contamination and support the notion that toxin-producing *Pseudo-nitzschia* species are nearly ubiquitous across global ocean basins. Thus, virtually the entire ocean is potentially at risk if climate change promotes increases in *Pseudo-nitzschia* growth and toxicity. Global models warn that increasingly prolific and toxic bloom events must be expected under a continuously warming ocean. These results are consistent with previous studies indicating that temperature plays a fundamental role in shaping latitudinal diversity patterns, species distributions, and metabolic activity across marine microbial communities. However, caution is warranted, as not all *Pseudo-nitzschia* species or strains produce more toxin under a warming ocean. For example, a strain of *P. australis* isolated from Washington state, USA, with an ambient seawater temperature of 14°C, showed higher toxin levels under cool water

conditions simulating upwelling (13°C, 900 μatm pCO$_2$, replete nutrients) than during heatwaves (19°C or 20.5°C, 900 μatm pCO$_2$, replete nutrients) (Zhu et al. 2017). In contrast, another strain of *P. australis* isolated from Southern California exhibited maximum toxin levels at 30°C (Sun et al. 2011). These variations likely stem from adaptation to local temperature regimes. To make accurate global predictions about DA production and harmful blooms, we need more research on the thermal responses of toxic *P. multiseries* strains from diverse geographical groups. Even so, our study provides a new basis for global assessments of toxic DA contamination risk to seafood safety under future climate change.

Conflicts of Interest

The authors declare no conflicts of interest.

Data Availability Statement

The data that support the findings of this study are freely available in Zenodo at https://doi.org/10.5281/zenodo.15813441. The sequencing data have been deposited in the NCBI database under accession number PRJNA1286142, PRJNA1286158, PRJNA1286141, PRJNA1286164, and PRJNA1286163. GFDL climate model data (SSP2-4.5) were obtained from the CMIP6 ESGF project at https://doi.org/10.22033/ESGF/CMIP6.8586.

References

Bates, S. S., K. A. Hubbard, N. Lundholm, M. Montresor, and C. P. Leaw. 2018. "*Pseudo-nitzschia*, *Nitzschia*, and Domoic Acid: New Research Since 2011." *Harmful Algae* 79: 3–43. https://doi.org/10.1016/j.hal.2018.06.001.

Boissonneault, K. R., B. M. Henningsen, S. S. Bates, et al. 2013. "Gene Expression Studies for the Analysis of Domoic Acid Production in the Marine Diatom *Pseudo-nitzschia multiseries*." *BMC Molecular Biology* 14, no. 25: 1–19. https://doi.org/10.1186/1471-2199-14-25.

Bowers, H. A., J. P. Ryan, K. Hayashi, et al. 2018. "Diversity and Toxicity of *Pseudo-nitzschia* Species in Monterey Bay: Perspectives From Targeted and Adaptive Sampling." *Harmful Algae* 78: 129–141. https://doi.org/10.1016/j.hal.2018.08.006.

Brunson, J. K., S. M. K. McKinnie, J. R. Chekan, et al. 2018. "Biosynthesis of the Neurotoxin Domoic Acid in a Bloom-Forming Diatom." *Science* 361, no. 6409: 1356–1358. https://doi.org/10.1126/science.aau0382.

Brunson, J. K., M. Thukral, J. P. Ryan, et al. 2024. "Molecular Forecasting of Domoic Acid During a Pervasive Toxic Diatom Bloom." *Proceedings of the National Academy of Sciences of the United States of America* 121, no. 40: e2319177121. https://doi.org/10.1101/2023.11.02.565333.

Callahan, B. J., P. J. McMurdie, M. J. Rosen, A. W. Han, A. J. A. Johnson, and S. P. Holmes. 2016. "DADA2: High-Resolution Sample Inference From Illumina Amplicon Data." *Nature Methods* 13, no. 7: 581–583. https://doi.org/10.1038/nmeth.3869.

Chen, J., J. Yang, X. He, et al. 2023. "Prevalence of the Neurotoxin Domoic Acid in the Aquatic Environments of the Bohai and Northern Yellow Seas in China." *Science of the Total Environment* 876: 162732. https://doi.org/10.1016/j.scitotenv.2023.162732.

Chen, S. 2023. "Ultrafast One-Pass FASTQ Data Preprocessing, Quality Control, and Deduplication Using Fastp." *iMeta* 2, no. 2: e107. https://doi.org/10.1002/imt2.107.

Clark, S., K. A. Hubbard, D. M. Anderson, D. J. McGillicuddy Jr., D. K. Ralston, and D. W. Townsend. 2019. "*Pseudo-nitzschia* Bloom Dynamics in the Gulf of Maine: 2012–2016." *Harmful Algae* 88: 101656. https://doi.org/10.1016/j.hal.2019.101656.

Dai, Y., S. Yang, D. Zhao, et al. 2023. "Coastal Phytoplankton Blooms Expand and Intensify in the 21st Century." *Nature* 615, no. 7951: 280–284. https://doi.org/10.1038/s41586-023-05760-y.

De Vargas, C., S. Audic, N. Henry, et al. 2015. "Eukaryotic Plankton Diversity in the Sunlit Ocean." *Science* 348, no. 6237: 1261605. https://doi.org/10.1126/science.1261605.

Delegrange, A., A. Lefebvre, F. Gohin, L. Courcot, and D. Vincent. 2018. "*Pseudo-nitzschia* sp. Diversity and Seasonality in the Southern North Sea, Domoic Acid Levels and Associated Phytoplankton Communities." *Estuarine, Coastal and Shelf Science* 214: 194–206. https://doi.org/10.1016/j.ecss.2018.09.030.

Dong, H. C., N. Lundholm, S. T. Teng, et al. 2020. "Occurrence of *Pseudo-nitzschia* Species and Associated Domoic Acid Production Along the Guangdong Coast, South China Sea." *Harmful Algae* 98: 101899. https://doi.org/10.1016/j.hal.2020.101899.

Edgar, R. C. 2013. "UPARSE: Highly Accurate OTU Sequences From Microbial Amplicon Reads." *Nature Methods* 10: 996–998. https://doi.org/10.1038/nmeth.2604.

Esenkulova, S., B. J. G. Sutherland, A. Tabata, N. Haigh, C. M. Pearce, and K. M. Miller. 2020. "Comparing Metabarcoding and Morphological Approaches to Identify Phytoplankton Taxa Associated With Harmful Algal Blooms." *Facets* 5, no. 1: 784–811. https://doi.org/10.1139/facets-2020-0025.

Eyring, V., S. Bony, G. A. Meehl, et al. 2016. "Overview of the Coupled Model Intercomparison Project Phase 6 (CMIP6) Experimental Design and Organization." *Geoscientific Model Development* 9, no. 5: 1937–1958. https://doi.org/10.5194/gmd-9-1937-2016.

Garcia, H. E., R. A. Locarnini, T. P. Boyer, et al. 2013. "World Ocean Atlas 2013." In *NOAA Atlas NESDIS*, edited by S. Levitus. U.S. Government Printing Office.

Guiry, M. D., and G. M. Guiry. 2021. *AlgaeBase. World-Wide Electronic Publication*. National University of Ireland. http://www.algaebase.org.

Hallegraeff, G. M., D. M. Anderson, C. Belin, et al. 2021. "Perceived Global Increase in Algal Blooms is Attributable to Intensified Monitoring and Emerging Bloom Impacts." *Communications Earth & Environment* 2, no. 1: 117. https://doi.org/10.1038/s43247-021-00178-8.

Hastie, T. J. 2017. "Generalized Additive Models." In *Statistical Models in S*, 249–307. Routledge.

Huang, C. X., H. C. Dong, N. Lundholm, et al. 2019. "Species Composition and Toxicity of the Genus *Pseudo-nitzschia* in Taiwan Strait, Including *P. chiniana* sp. nov. and *P. qiana* sp. nov." *Harmful Algae* 84: 195–209. https://doi.org/10.1016/j.hal.2019.04.003.

Ibarbalz, F. M., N. Henry, M. C. Brandão, et al. 2019. "Global Trends in Marine Plankton Diversity Across Kingdoms of Life." *Cell* 179, no. 5: 1084–1097. https://doi.org/10.1016/j.cell.2019.10.008.

Jabre, L. J., A. E. Allen, J. S. P. McCain, et al. 2021. "Molecular Underpinnings and Biogeochemical Consequences of Enhanced Diatom Growth in a Warming Southern Ocean." *Proceedings of the National Academy of Sciences* 118, no. 30: e2107238118. https://doi.org/10.1073/pnas.2107238118.

Kelly, K. J., A. Mansour, C. Liang, et al. 2023. "Simulated Upwelling and Marine Heatwave Events Promote Similar Growth Rates but Differential Domoic Acid Toxicity in *Pseudo-nitzschia australis*." *Harmful Algae* 127: 102467. https://doi.org/10.1016/j.hal.2023.102467.

Kling, J. D., M. D. Lee, F. Fu, et al. 2020. "Transient Exposure to Novel High Temperatures Reshapes Coastal Phytoplankton Communities." *ISME Journal* 14, no. 2: 413–424. https://doi.org/10.1038/s41396-019-0525-6.

Lefebvre, K. A., and A. Robertson. 2010. "Domoic Acid and Human Exposure Risks: A Review." *Toxicon* 56, no. 2: 218–230. https://doi.org/10.1016/j.toxicon.2009.05.034.

Lelong, A., H. Hégaret, P. Soudant, and S. S. Bates. 2012. "*Pseudo-nitzschia* (Bacillariophyceae) Species, Domoic Acid and Amnesic Shellfish Poisoning: Revisiting Previous Paradigms." *Phycologia* 51, no. 2: 168–216. https://doi.org/10.2216/11-37.1.

Lu, J., F. P. Breitwieser, P. Thielen, and S. L. Salzberg. 2017. "Bracken: Estimating Species Abundance in Metagenomics Data." *PeerJ Computer Science* 3: e104. https://doi.org/10.7717/peerj-cs.104.

Lü, S., Y. Li, N. Lundholm, Y. Ma, and K. C. Ho. 2012. "Diversity, Taxonomy and Biogeographical Distribution of the Genus *Pseudo-nitzschia* (Bacillariophyceae) in Guangdong Coastal Waters, South China Sea." *Nova Hedwigia* 95: 123–152. https://doi.org/10.1127/0029-5035/2012/0046.

Lundholm, N., C. Churro, L. Escalera, et al. 2009. "IOC-UNESCO Taxonomic Reference List of Harmful Micro Algae." https://www.marinespecies.org/hab. https://doi.org/10.14284/362.

Lundholm, N., A. Clarke, and M. Ellegaard. 2010. "A 100-Year Record of Changing *Pseudo-nitzschia* Species in a Sill-Fjord in Denmark Related to Nitrogen Loading and Temperature." *Harmful Algae* 9, no. 5: 449–457. https://doi.org/10.1016/j.hal.2010.03.001.

Magoč, T., and S. L. Salzberg. 2011. "FLASH: Fast Length Adjustment of Short Reads to Improve Genome Assemblies." *Bioinformatics* 27, no. 21: 2957–2963. https://doi.org/10.1093/bioinformatics/btr507.

Masella, A. P., A. K. Bartram, J. M. Truszkowski, D. G. Brown, and J. D. Neufeld. 2012. "PANDAseq: Paired-End Assembler for Illumina Sequences." *BMC Bioinformatics* 13: 31. https://doi.org/10.1186/1471-2105-13-31.

McCabe, R. M., B. M. Hickey, R. M. Kudela, et al. 2016. "An Unprecedented Coastwide Toxic Algal Bloom Linked to Anomalous Ocean Conditions." *Geophysical Research Letters* 43, no. 19: 10366–10376. https://doi.org/10.1002/2016GL070023.

Moon, J. Y., K. Lee, W. A. Lim, et al. 2021. "Anthropogenic Nitrogen is Changing the East China and Yellow Seas From Being N Deficient to Being P Deficient." *Limnology and Oceanography* 66, no. 3: 914–924. https://doi.org/10.1002/lno.11651.

Obiol, A., C. R. Giner, P. Sánchez, C. M. Duarte, S. G. Acinas, and R. Massana. 2020. "A Metagenomic Assessment of Microbial Eukaryotic Diversity in the Global Ocean." *Molecular Ecology Resources* 20, no. 3: 718–731. https://doi.org/10.1111/1755-0998.13147.

Pierella Karlusich, J. J., K. Cosnier, L. Zinger, et al. 2025. "Patterns and Drivers of Diatom Diversity and Abundance in the Global Ocean." *Nature Communications* 16, no. 1: 3452. https://doi.org/10.1038/s41467-025-58027-7.

Radan, R. L., and W. P. Cochlan. 2018. "Differential Toxin Response of *Pseudo-nitzschia multiseries* as a Function of Nitrogen Speciation in Batch and Continuous Cultures, and During a Natural Assemblage Experiment." *Harmful Algae* 73: 12–29. https://doi.org/10.1016/j.hal.2018.01.002.

Rynearson, T. A., S. A. Flickinger, and D. N. Fontaine. 2020. "Metabarcoding Reveals Temporal Patterns of Community Composition and Realized Thermal Niches of *Thalassiosira* spp. (Bacillariophyceae) From the Narragansett Bay Long-Term Plankton Time Series." *Biology* 9, no. 1: 19. https://doi.org/10.3390/biology9010019.

Schnetzer, A., P. E. Miller, R. A. Schaffner, et al. 2007. "Blooms of *Pseudo-nitzschia* and Domoic Acid in the San Pedro Channel and Los Angeles Harbor Areas of the Southern California Bight, 2003–2004." *Harmful Algae* 6, no. 3: 372–387. https://doi.org/10.1016/j.hal.2006.11.004.

Scholin, C. A., F. Gulland, G. J. Doucette, et al. 2000. "Mortality of Sea Lions Along the Central California Coast Linked to a Toxic Diatom Bloom." *Nature* 403, no. 6765: 80–84. https://doi.org/10.1038/47481.

Sekula-Wood, E., A. Schnetzer, C. R. Benitez-Nelson, et al. 2009. "Rapid Downward Transport of the Neurotoxin Domoic Acid in Coastal Waters." *Nature Geoscience* 2, no. 4: 272–275. https://doi.org/10.1038/ngeo472.

Silver, M. W., S. Bargu, S. L. Coale, et al. 2010. "Toxic Diatoms and Domoic Acid in Natural and Iron Enriched Waters of the Oceanic Pacific." *Proceedings of the National Academy of Sciences* 107, no. 48: 20762–20767. https://doi.org/10.1073/pnas.1006968107.

Sun, J., D. A. Hutchins, Y. Feng, E. L. Seubert, D. A. Caron, and F. X. Fu. 2011. "Effects of Changing pCO_2 and Phosphate Availability on Domoic Acid Production and Physiology of the Marine Harmful Bloom Diatom *Pseudo-nitzschia multiseries*." *Limnology and Oceanography* 56, no. 3: 829–840. https://doi.org/10.4319/lo.2011.56.3.0829.

Trainer, V. L., S. S. Bates, N. Lundholm, et al. 2012. "*Pseudo-nitzschia* Physiological Ecology, Phylogeny, Toxicity, Monitoring and Impacts on Ecosystem Health." *Harmful Algae* 14: 271–300. https://doi.org/10.1016/j.hal.2011.10.025.

Trick, C. G., B. D. Bill, W. P. Cochlan, M. L. Wells, V. L. Trainer, and L. D. Pickell. 2010. "Iron Enrichment Stimulates Toxic Diatom Production in High-Nitrate, Low-Chlorophyll Areas." *Proceedings of the National Academy of Sciences* 107, no. 13: 5887–5892. https://doi.org/10.1073/pnas.0910579107.

Wang, J., J. Chen, J. Yang, et al. 2021. "Determination of Domoic Acid in Seawater by Solid Phase Extraction-Liquid Chromatography-Tandem Mass Spectrometry." *Chinese Journal of Chromatography* 39, no. 8: 889–895. https://doi.org/10.3724/SP.J.1123.2021.02026.

Wang, Z., L. Liu, Y. Tang, et al. 2022. "Phytoplankton Community and HAB Species in the South China Sea Detected by Morphological and Metabarcoding Approaches." *Harmful Algae* 118: 102297. https://doi.org/10.1016/j.hal.2022.102297.

Wang, Z., J. Maucher-Fuquay, S. E. Fire, et al. 2012. "Optimization of Solid-Phase Extraction and Liquid Chromatography-Tandem Mass Spectrometry for the Determination of Domoic Acid in Seawater, Phytoplankton, and Mammalian Fluids and Tissues." *Analytica Chimica Acta* 715: 71–79. https://doi.org/10.1016/j.aca.2011.12.013.

Xu, D., G. Zheng, G. Brennan, et al. 2023. "Plastic Responses Lead to Increased Neurotoxin Production in the Diatom *Pseudo-nitzschia* Under Ocean Warming and Acidification." *ISME Journal* 17, no. 4: 525–536. https://doi.org/10.1038/s41396-023-01370-8.

Zhu, F., R. Massana, F. Not, D. Marie, and D. Vaulot. 2005. "Mapping of Picoeucaryotes in Marine Ecosystems With Quantitative PCR of the 18S rRNA Gene." *FEMS Microbiology Ecology* 52, no. 1: 79–92. https://doi.org/10.1016/j.femsec.2004.10.006.

Zhu, Z., P. Qu, F. Fu, N. Tennenbaum, A. O. Tatters, and D. A. Hutchins. 2017. "Understanding the Blob Bloom: Warming Increases Toxicity and Abundance of the Harmful Bloom Diatom *Pseudo-nitzschia* in California Coastal Waters." *Harmful Algae* 67: 36–43. https://doi.org/10.1016/j.hal.2017.06.004.

Supporting Information

Additional supporting information can be found online in the Supporting Information section. **Data S1.**